Current Biology, Vol. 14, 1410–1414, August 10, 2004, ©2004 Elsevier Ltd. All rights reserved. DOI 10.1016/j.cub.2004.06.065

Arabidopsis NAP1 Is Essential for Arp2/3-Dependent Trichome Morphogenesis

Michael J. Deeks,[1,4] Despina Kaloriti,[1,4] Brendan Davies,[2] Rui Malhó,[3] and Patrick J. Hussey[1,*]

[1]The Integrative Cell Biology Laboratory
School of Biological and Biomedical Sciences
University of Durham
South Road
Durham DH1 3LE
United Kingdom

[2]Leeds Institute of Plant Biotechnology and Agriculture
University of Leeds
Clarendon Way
Leeds LS2 9JT
United Kingdom

[3]Universidade de Lisboa
Faculdade Ciências
Instituto Ciência Aplicada e Tecnologia
Lisbon
Portugal

Summary

The dynamic nature of the eukaryotic actin cytoskeleton is essential for the locomotion of animal cells and the morphogenesis of plant and fungal cells. The F-actin nucleating/branching activity of the Arp2/3 complex is a key function for all of these processes. The SCAR/WAVE family represents a group of Arp2/3 activators that are associated with lamellipodia formation [1, 2]. A protein complex of PIR121, NAP1, ABI, and HSPC300 is required for SCAR regulation by cell signaling pathways [3], but the exact nature of this interaction is controversial and represents a continually evolving model [4]. The mechanism originally proposed was of a SCAR *trans* repressing complex supported by evidence from in vitro experiments [3]. This model was reinforced by genetic studies in the *Drosophila* central nervous system [5] and *Dictyostelium* [6], where the knockout of certain SCAR-complex components leads to excessive SCAR-mediated actin polymerization. Conflicting data have steadily accumulated from animal tissue culture experiments suggesting that the complex activates rather than represses in vivo SCAR activity [7–9]. Recent biochemical evidence supports the SCAR-complex activator model [9]. Here, we show that genetic observations in *Arabidopsis* are compatible with an activation model and provide one potential mechanism for the regulation of the newly identified *Arabidopsis* Arp2/3 complex.

Results and Discussion

Five alleles representing T-DNA inserts into *AtNAP1* (*Arabidopsis thaliana* homolog of Nck-Associated Protein 1) were identified from the SALK T-DNA collection: *nap1-1* through *nap1-5*. Three alleles show an insert into exons, one allele has an insert in an intron, and one allele has an insert within the 5′ UTR (Figure 1A). Allelism was confirmed through absence of complementation ($n > 40$ for each allele). The insertion of a T-DNA in allele *nap1-1* (Figure 1B) and *nap1-2* has created stop codons that effectively truncate the protein to one quarter of its original length. The presence of stop codons within the transcript of *nap1-1* was confirmed by the sequencing of mutant allele RT-PCR product. *Drosophila nap1/kette* alleles with stop codons in equivalent N terminus positions to *nap1-1* and *-2* constitute null alleles [10] (see Figure S1); therefore, despite no phenotypic difference having been detected between the *Arabidopsis* alleles, all further analysis was performed with putative null allele *nap1-1*.

The trichomes of *nap1* allele homozygotes physically resemble the *distorted* phenotype of trichomes of Arp2/3 component null alleles [11–15] and have the morphology of trichomes grown in the presence of actin-depolymerizing drugs [16, 17]. The development of trichomes was compared in *nap1-1* homozygotes, *arp2-1* homozygotes (SALK allele 010045), the double mutant, and the wild-type with ESEM imaging of critical-point dried rosettes fixed 7 days after germination (DAG) (Figure 1C). Trichome development can be divided into six stages based upon changes in the mode of growth. It has previously been reported that the distorted phenotype of *arp2/3* mutants becomes manifest at stage 4 during branch extension [13]. ESEM imaging showed that *nap1-1* trichomes initiated defective growth at stage 4 in conjunction with *arp2-1* trichomes (see Figure S2 in the Supplemental Data available with this article online). Double-mutant homozygote trichomes resemble single-mutant phenotypes (Figure 1C), supporting the hypothesis that *ARP2* and *NAP1* function in the same trichome developmental pathway.

Arabidopsis plants homozygous for mutants of *arp2*, *arp3*, *arpC2*, and *arpC5* have been shown to exhibit defects in the organization of the trichome F-actin cytoskeleton. Figure 2A compares trichome F-actin in *nap1-1* plants to that in *arp2-1* and wild-type plants in a cross with a line stably expressing GFP:FABD [18] and via freeze shattering followed by staining with anti-actin antibody. Both anti-actin antibodies and GFP:FABD showed an intact *nap1* F-actin cytoskeleton similar to descriptions of distorted-class mutants from previously published experiments using live phalloidin uptake and anti-actin staining [13, 15] but not to those using GFP-talin. [11, 12, 17]. Actin cables are present in both *nap1* and *arp2* mutant trichomes but show a higher level of disorganization when compared to wild-type cables during stage 4 of development onward.

In other organisms, exploitation of the role of the Arp2/3 complex as a nucleator of F-actin polymerization has allowed researchers to infer the level of Arp2/3 activation in *nap1* mutant backgrounds by assessing the level of F-actin accumulation in the cytoplasm. Single

*Correspondence to p.j.hussey@durham.ac.uk
[4]These authors contributed equally to this work.

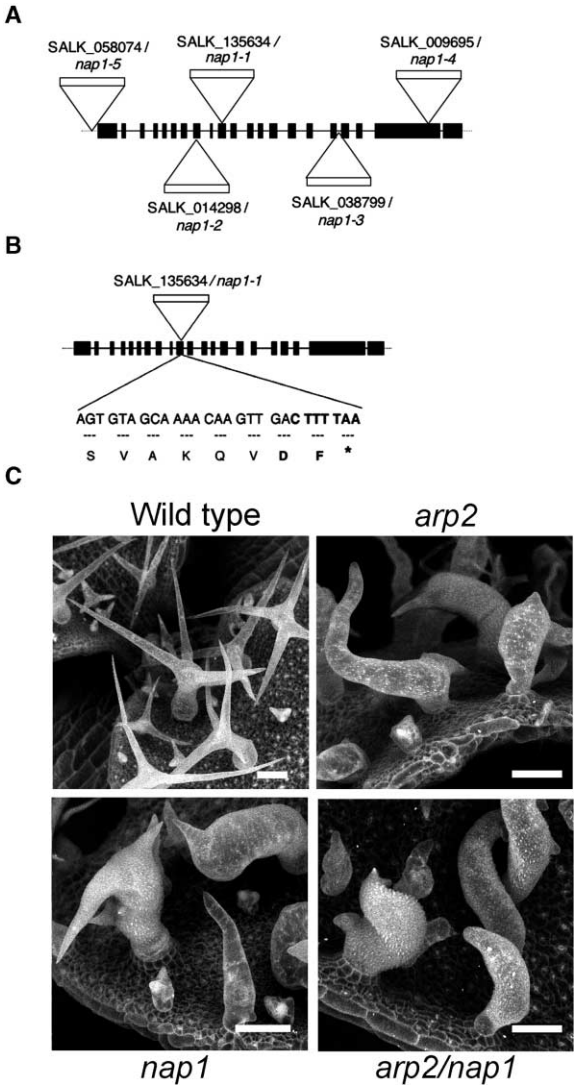

Figure 1. The *nap1* Alleles and the *nap1-1* and *arp2-1* Trichome Phenotype

(A) Sequencing Kazusa cDNA clone RZL04d02R confirmed the *AtNAP1* (At2g35110) splice pattern. Exons are presented as solid boxes. The position of each T-DNA allele is shown.

(B) The T-DNA insertion into allele *nap1-1* generates a premature stop codon. The T-DNA sequence of *nap1-1* and the insert-specific amino acid sequence are in bold.

(C) ESEM pictures of leaves 7 days after seedling germination (DAG) show trichomes of wild-type, *arp2* and *nap1* mutants, and the double mutant. No morphological differences at any stage of development between *nap1* and *arp2* trichomes were detected.

All scale bars represent 50 μm.

branched F-actin filaments have, to date, not been observed in plant cells. Imaging of trichomes expressing GFP:FABD and stained with antibodies can only resolve actin bundles that probably contain many parallel filaments. F-actin levels at the cortex of stage 4/5 branches of *nap1*, *arp2*, and wild-type trichomes were assessed by counting the number of bundles that transect the midpoint of the branch cortex (Figure 2B). The number of cables per unit width of cortex observed is slightly reduced in *arp2* and *nap1* mutants. Importantly, no excessive F-actin accumulation can be observed in *Arabidopsis nap1* mutant trichomes, as has been reported in *Drosophila nap1* mutants [5].

The ratio of subcortical "core" actin to total actin abundance was found to differ in stage 4/5 *arpC2* and *arp3* trichomes versus wild-type trichomes of a similar developmental stage [13, 15]. Figure 2C shows the core-to-total ratios of *nap1* and *arp2* mutant trichomes as compared to that of the wild-type. GFP:FABD crosses were used because trichomes did not suffer mechanical damage during sample preparation. The ratio of core fluorescence to total fluorescence for *arp2* shows a mild reduction with respect to the wild-type, suggesting that the subcortical core of stage 4/5 trichomes is relatively depleted of actin. The stage 4/5 branches of *nap1-1* trichomes show an intermediate ratio. As compared to the actin cables in the trichome cytoplasm of the Arp2/3 complex mutants, the actin cables of *nap1* plants may suffer from a similar but less severe rearrangement within the trichome cytoplasm.

In animal cells, NAP1 protein does not interact directly with the Arp2/3 complex. NAP1 binds to the N terminus of Abl-interacting (ABI) proteins that are also bound to SCAR/WAVE family proteins [9, 19]. *Arabidopsis* retains families of ABI-like proteins (see Figure S3) and Scar Homology Domain (SHD) proteins [20]. Four *Arabidopsis* SHD proteins contain a VCA-like sequence at their C terminus, where residues critical for the interaction with actin monomers and for Arp2/3 activation [21] have been conserved (Figure 3A). The ability of the *Arabidopsis* WH2 domain to bind G-actin was confirmed by expression of the VCA region of the SCAR-like protein AtSCAR1 (At2g34150), fused to a GST tag. The VCA protein bound to glutathione-sepharose beads was incubated with a Tobacco BY2 cell extract. Polyacrylamide gel electrophoresis followed by Western blotting and probing with anti-actin showed that actin associates with the VCA region (Figure 3B), suggesting that *Arabidopsis* SHD proteins could function as SCAR orthologs (Figure 4).

Our observations of trichome morphology and trichome F-actin organization are consistent with a role for NAP1 as an activator of the Arp2/3 complex. Potentially, an over-active Arp2/3 complex caused by the deactivation of NAP1 could also cause severe disruption to plant cell morphogenesis, but it seems unlikely that this would precisely phenocopy known Arp2/3 component mutations. Similarity in phenotypes between Arp2/3 mutants and *nap1* extends beyond trichomes to other tissues, including hypocotyls grown under dark conditions (see Figure S4). It is not possible to compare the *Arabidopsis nap1* phenotype to constitutively active Arp2/3 because overexpression of Arp2/3-stimulating proteins in vivo has been shown to have non-Arp2/3-related gain-of-function effects [22] and dominant-negative phenotypes [1]. In the absence of further knowledge, the most likely model for NAP1 function in *Arabidopsis* is as an activator of the Arp2/3 complex. The discrepancy between the *Arabidopsis* phenotype and the *Drosophila* central nervous system agrees with the theory that a particular cell-type's response to the loss of a SCAR-complex member depends on multiple factors, such as SCAR protein degradation, SCAR localization, and actin dynamics [4]. The potential retention

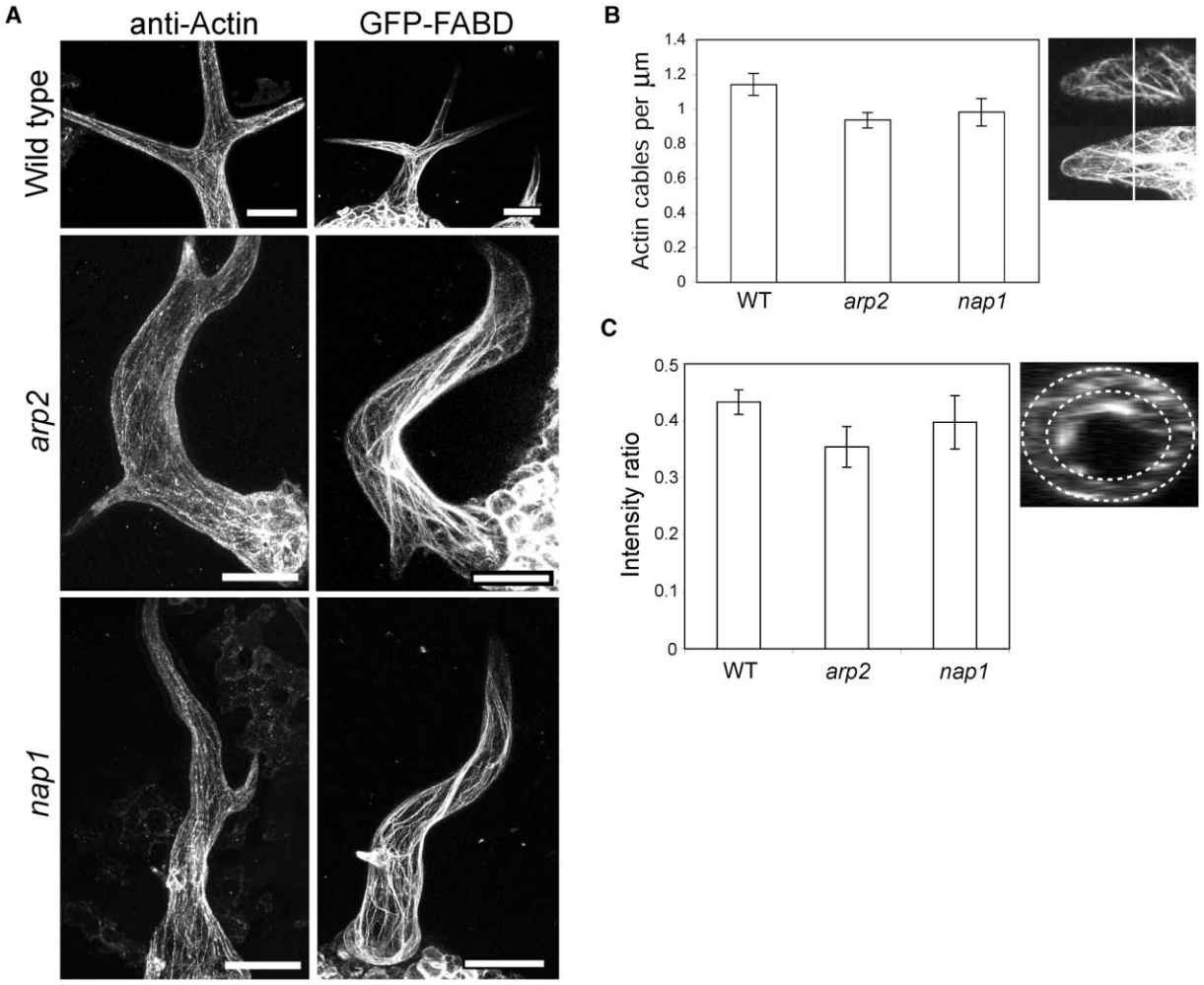

Figure 2. The Actin Cytoskeleton of Wild-Type, *arp2*, and *nap1* Trichomes

(A) Total projection of stage 6 mature trichomes. The actin network was visualized with anti-actin staining and GFP:FABD.

(B) Quantitation of actin cables transecting the midpoint of stage 4/5 branches within a 2.5-μm-deep section of the cortex.

(C) Calculation of the ratio of core actin (defined as actin within a perimeter 2.5 μm from the cell surface: actin in the inner circle) in stage 4/5 trichomes to total cross-sectional levels of actin in GFP:FABD trichome branches.

of a plant-customized SCAR complex by *Arabidopsis* (Figure 4B) offers an additional route to learn how this group of proteins localizes and activates actin polymerization.

Experimental Procedures

Plant Material

Insertion lines *arp2-1* and *nap1-1* to *-5* were generated by The Salk Institute Genomic Analysis Laboratory in *Arabidopsis* ecotype Col–0 with T-DNA insertion vector pROK 2. Plant genotypes were identifed by PCR, and T4 homozygotes were used throughout. *Arabidopsis* ecotype Col-0 T3 seeds harboring GFP:FABD [18] were used for crosses to the *arp2* and *nap1* homozygote lines. Plants for microscopy analysis were grown on half MS salts, 0.8% (w/v) plant agar.

Microscopy

ESEM samples were prepared by fixation (PBS, 1% glutaldehyde, 0.1% Tween) and dehydration by an ethanol series followed by critical-point drying with carbon dioxide. Freeze shattering of trichomes and anti-actin (C4, ICN) staining were conducted as described in [16]. All fluorescence microscopy was performed with a Zeiss LSM510 confocal microscope. So that the abundance of F-actin structures could be assessed (Figure 2B), the number of cables transecting the midpoint of stage 4/5 branches within a 2.5-μm-deep section of the cortex were counted. The number of cables was divided by the width of the cortex at the midpoint so that the number of cables per micron could be counted. The ratio of core actin (defined as actin within a perimeter 2.5 μm from the cell surface) in stage 4/5 trichomes was compared to total cross-sectional levels of actin via z axis projections of GFP:FABD trichome branches (Figure 2C). Open Lab image analysis software (Improvision) was used for measuring the fluorescence intensity of branch cross-sections. Sixteen branches for wild-type, 12 branches for *arp2*, and 11 branches for *nap1* were analyzed.

Protein Expression

The VCA domain of AtSCAR1 (accession number BK005566) comprising amino acids 681–822 was cloned into the GST fusion vector pGEX-4T-1 and expressed in Rosetta 2 (DE3) pLysS (Novagen) bacterial cells. Recombinant GST-VCA and GST alone as a control were purified with glutathione sepharose 4B resin (Amersham).

Actin Binding Assay

Ten milliliters of 5-day-old Tobacco BY2 suspension culture cell culture was harvested by centrifugation, and the cells were frozen in liquid nitrogen and ground with a mortar and pestle. The frozen

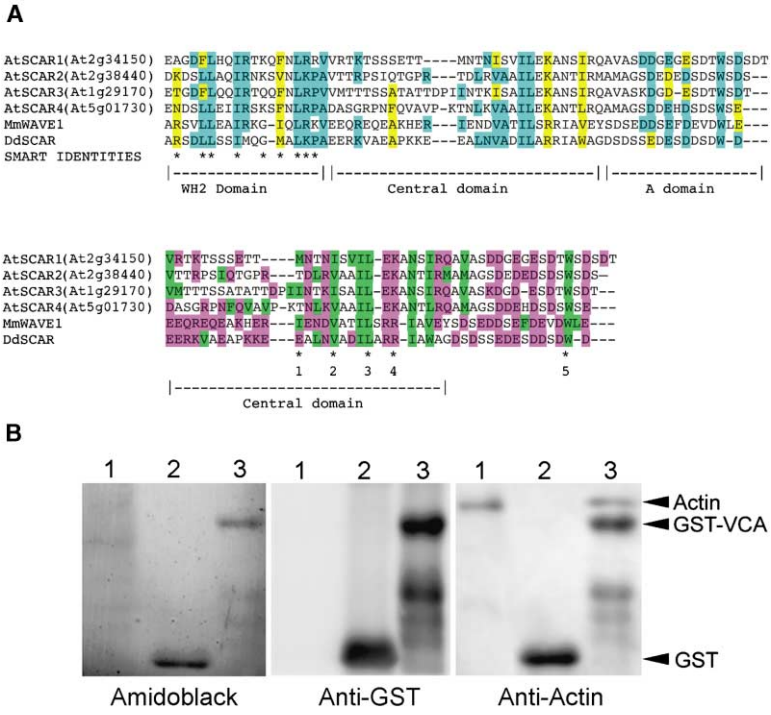

Figure 3. *Arabidopsis* SCAR/WAVE-like Proteins

(A) ClustalX alignments of SCAR C termini. In the upper alignment, *Arabidopsis* residues identical to either WAVE1 (Mouse) or SCAR (Dictyostelium) are highlighted blue. Similar residues are highlighted yellow. The alignment has been divided into the WH2 domain, central domain, and acidic domain. Residues marked with an asterisk within the WH2 domain correspond to residues with >60% identity within the SMART pile-up used for generating the SMART HMM for WH2. The majority of these residues are conserved within the *Arabidopsis* homologs. The lower alignment of the central and acidic domains compares hydrophobicity. Panchal et al. identified a conserved amphipathic helix within the central domain critical for WASP/SCAR activation of the Arp2/3 complex [21]. The residues conserved within animal SCAR family members have been numbered below the alignment. Hydrophobic residues are highlighted green, and polar residues are highlighted purple. Hydrophobic positions 2 and 3 are conserved in all plant SCAR homologs. Arginine at position 4 has been replaced by another basic residue, lysine. The tryptophan residue within the acidic domain (position 5) is required for SCAR to bind to the Arp2/3 complex [21, 23].

(B) Western blot of GST pull-down experiments using GST-VCA attached to glutathione sepharose 4B beads incubated in Tobacco BY2 cell extract. Lane 1: total cell extract. Lane 2: GST beads pelleted from the total cell extract. Lane 3: GST-VCA beads pelleted from the total cell extract. The blot was stained with Amido black and probed with anti-GST. The same blot was probed with anti-actin.

material was resuspended in 10 ml of 2 × PBS and 0.4% Tween-20, containing a cocktail of protease inhibitors (20 mM PMSF, 20 μg/ml Aprotinin, 20 μg/ml Leupeptin, 20 μg/ml TAME, and 20 μg/ml pepstatin). The extract was incubated at 4°C with 5 μg of GST-VCA attached to glutathione sepharose 4B resin. Control GST and beads alone were incubated in parallel. The samples were fractionated on one-dimensional polyacrylamide gels. Western blots were probed with anti-GST (Amersham) and anti-actin antibody C4 (ICN) as described in [18].

Supplemental Data

Four supplemental figures are available with this article online at http://www.current-biology.com/cgi/content/full/14/15/1410/DC1/.

Acknowledgments

We would like to thank Tijs Ketelaar and Andrei Smertenko for useful discussions through the course of this project. This work was supported by the Biotechnology and Biological Sciences Research Council UK (M.J.D., B.D., and P.J.H.) and the EU human potential program, TIPNET HPRN-CT-2002-00265 (D.K., R.M., and P.J.H.).

Received: April 23, 2004
Revised: June 18, 2004
Accepted: June 21, 2004
Published online: July 1, 2004

References

1. Machesky, L.M., and Insall, R.H. (1998). Scar1 and the related Wiskott-Aldrich syndrome protein, WASP, regulate the actin cytoskeleton through the Arp2/3 complex. Curr. Biol. *8*, 1347–1356.
2. Machesky, L.M., Mullins, R.D., Higgs, H.N., Kaiser, D.A., Blanchoin, L., May, R.C., Hall, M.E., and Pollard, T.D. (1999). Scar, a WASp-related protein, activates nucleation of actin filaments by the Arp2/3 complex. Proc. Natl. Acad. Sci. USA *96*, 3739–3744.
3. Eden, S., Rohatgi, R., Podtelejnikov, A.V., Mann, M., and Kirschner, M.W. (2002). Mechanism of regulation of WAVE1-induced actin nucleation by Rac1 and Nck. Nature *418*, 790–793.
4. Blagg, S.L., and Insall, R.H. (2004). Solving the WAVE function. Nat. Cell Biol. *6*, 279–281.
5. Bogdan, S., and Klambt, C. (2003). Kette regulates actin dynamics and genetically interacts with Wave and Wasp. Development *130*, 4427–4437.
6. Blagg, S.L., Stewart, M., Sambles, C., and Insall, R.H. (2003). PIR121 regulates pseudopod dynamics and SCAR activity in Dictyostelium. Curr. Biol. *13*, 1480–1487.
7. Kunda, P., Craig, G., Dominguez, V., and Baum, B. (2003). Abi, Sra1, and Kette control the stability and localization of SCAR/WAVE to regulate the formation of actin-based protrusions. Curr. Biol. *13*, 1867–1875.
8. Steffen, A., Rottner, K., Ehinger, J., Innocenti, M., Scita, G., Wehland, J., and Stradal, T.E. (2004). Sra-1 and Nap1 link Rac to actin assembly driving lamellipodia formation. EMBO J. *23*, 749–759.
9. Innocenti, M., Zucconi, A., Disanza, A., Frittoli, E., Areces, L.B., Steffen, A., Stradal, T.E., Fiore, P.P., Carlier, M.F., and Scita, G. (2004). Abi1 is essential for the formation and activation of a WAVE2 signalling complex. Nat. Cell Biol. *6*, 319–327.
10. Hummel, T., Leifker, K., and Klambt, C. (2000). The Drosophila HEM-2/NAP1 homolog KETTE controls axonal pathfinding and cytoskeletal organization. Genes Dev. *14*, 863–873.
11. Mathur, J., Mathur, N., Kirik, V., Kernebeck, B., Srinivas, B.P., and Hulskamp, M. (2003). Arabidopsis CROOKED encodes for the smallest subunit of the ARP2/3 complex and controls cell shape by region specific fine F-actin formation. Development *130*, 3137–3146.
12. Mathur, J., Mathur, N., Kernebeck, B., and Hulskamp, M. (2003). Mutations in actin-related proteins 2 and 3 affect cell shape development in Arabidopsis. Plant Cell *15*, 1632–1645.
13. Le, J., El-Din El-Assal, S., Basu, D., Saad, M.E., and Szymanski, D.B. (2003). Requirements for Arabidopsis ATARP2 and ATARP3 during epidermal development. Curr. Biol. *13*, 1341–1347.
14. Li, S., Blanchoin, L., Yang, Z., and Lord, E.M. (2003). The putative

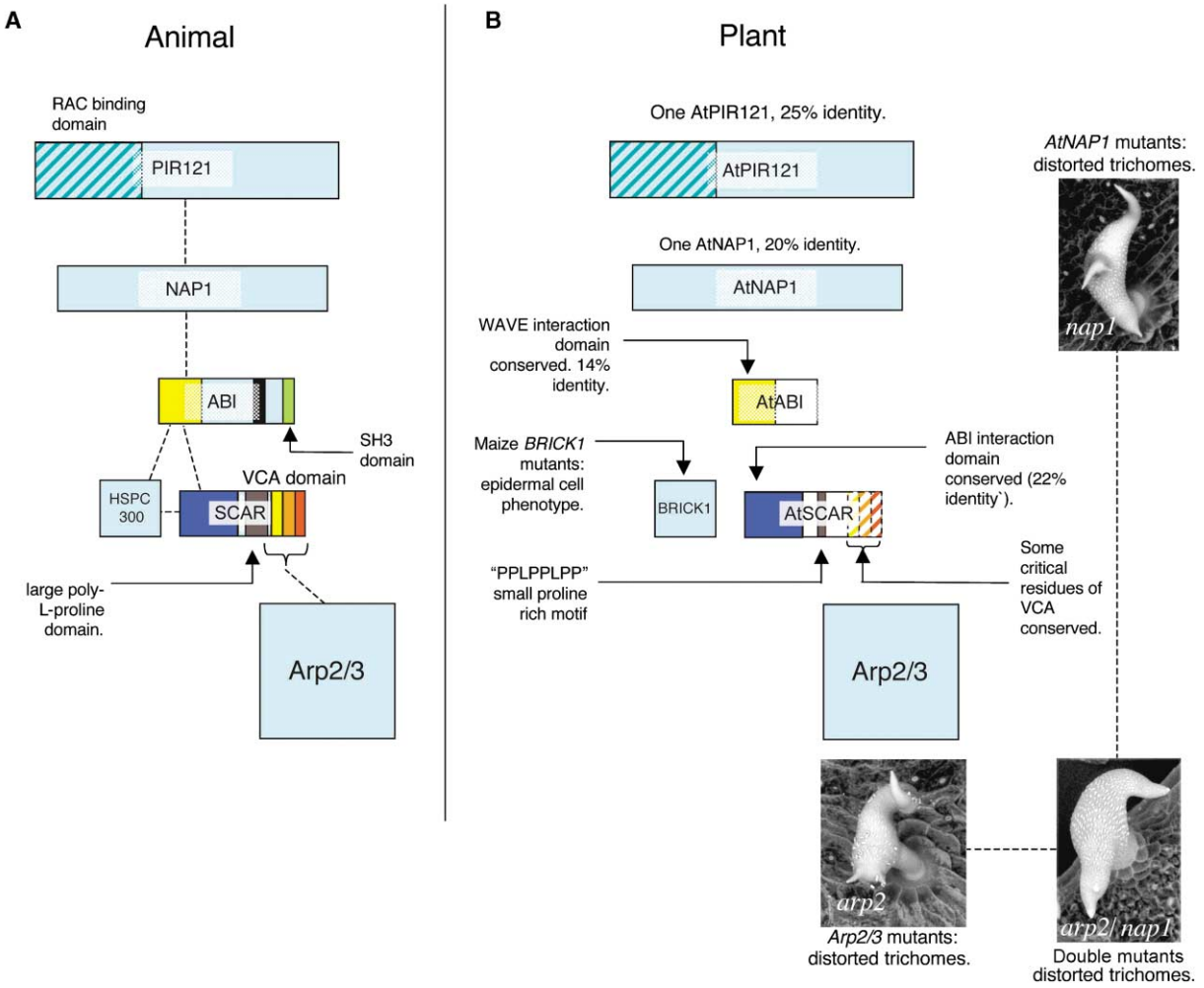

Figure 4. Comparison of the Animal SCAR Complex and Putative Plant SCAR Complex

Components of the complex are arranged as described by Innocenti et al. [9] and Gautreau et al. [19]. Characterized protein interactions are shown as dashed lines. The hatched section of PIR121 denotes a 407 amino acid RAC binding domain. The SCAR/WAVE conserved SCAR homology domain (SHD) required for the localization of SCAR and for interaction with ABI is colored blue. ABI localization domains are colored yellow. Poly-L-proline regions are colored black. Unspecific sections of primary amino acid sequence not conserved in the plant homologs are represented by absence of color. Individual trichome ESEM micrographs show the similarity in phenotype between *nap1,arp2* and *arp2/nap1* mutants in this pathway.

Arabidopsis arp2/3 complex controls leaf cell morphogenesis. Plant Physiol. *132*, 2034–2044.

15. El-Din El-Assal, S., Le, J., Basu, D., Mallery, E.L., and Szymanski, D.B. (2004). DISTORTED2 encodes an ARPC2 subunit of the putative Arabidopsis ARP2/3 complex. Plant J. *38*, 526–538.
16. Szymanski, D.B., Marks, M.D., and Wick, S.M. (1999). Organized F-actin is essential for normal trichome morphogenesis in Arabidopsis. Plant Cell *11*, 2331–2347.
17. Mathur, J., Spielhofer, P., Kost, B., and Chua, N. (1999). The actin cytoskeleton is required to elaborate and maintain spatial patterning during trichome cell morphogenesis in Arabidopsis thaliana. Development *126*, 5559–5568.
18. Ketelaar, T., Allwood, E.G., Anthony, R., Voigt, B., Menzel, D., and Hussey, P.J. (2004). The actin-interacting protein AIP1 is essential for actin organization and plant development. Curr. Biol. *14*, 145–149.
19. Gautreau, A., Ho, H.Y., Li, J., Steen, H., Gygi, S.P., and Kirschner, M.W. (2004). Purification and architecture of the ubiquitous Wave complex. Proc. Natl. Acad. Sci. USA *101*, 4379–4383.
20. Deeks, M.J., and Hussey, P.J. (2003). Arp2/3 and 'the shape of things to come'. Curr. Opin. Plant Biol. *6*, 561–567.
21. Panchal, S.C., Kaiser, D.A., Torres, E., Pollard, T.D., and Rosen, M.K. (2003). A conserved amphipathic helix in WASP/Scar proteins is essential for activation of Arp2/3 complex. Nat. Struct. Biol. *10*, 591–598.
22. Sasaki, N., Miki, H., and Takenawa, T. (2000). Arp2/3 complex-independent actin regulatory function of WAVE. Biochem. Biophys. Res. Commun. *272*, 386–390.
23. Marchand, J.B., Kaiser, D.A., Pollard, T.D., and Higgs, H.N. (2001). Interaction of WASP/Scar proteins with actin and vertebrate Arp2/3 complex. Nat. Cell Biol. *3*, 76–82.

Accession Numbers

The Genbank accession number for the AtSCAR1 gene is BK005566.